Applied Chemical Engineering (2023) Volume 6 Issue 1
doi:10.24294/ace.v6i1.1998

ORIGINAL RESEARCH ARTICLE

Photodegradation of Methylene blue and Rhodamine B using potato starch mediated zinc oxide nanoparticles and its calcium nanocomposites: Greener approach

Darshan Singh[1*], Anuradha[1], Surendra Kumar[2], Amar Kumar[3], Neelu Dheer[4], M. Ramananda Singh[5], Rajni Kanojia[6], Sangeeta Kaul[7], Ishwar Prasad Sahu[8]

[1] *Department of Chemistry, Daulat Ram College, University of Delhi, North Delhi 110007, India. E-mail: darshnachem2004@gmail.com; darshan@dr.du.ac.in*
[2] *Department of Chemistry, Hansraj College, University of Delhi, North Delhi 110007, India.*
[3] *Department of Chemistry, Ram Krishna Dwarika College, Patliputra University, Patna 800020, India.*
[4] *Department of Chemistry, Acharya Narendra Dev College, University of Delhi, North Delhi 110007, India.*
[5] *Department of Chemistry, Kirori Mal College, University of Delhi, North Delhi 110007, India.*
[6] *Department of Chemistry, Shivaji College, University of Delhi, North Delhi 110007, India.*
[7] *Department of Chemistry, Sri Aurobindo College, University of Delhi, North Delhi 110007, India.*
[8] *Department of Physics, Indira Gandhi National Tribal University, Amarkantak, Anuppur, Madhya Pradesh 484887, India.*

ABSTRACT

Zinc oxide is considered an effective photocatalyst for degradation of several organic contaminants found in wastewater. This work reports the biological synthesis of zinc oxide nanoparticles and its calcium nanocomposites to study the photocatalytic deterioration of two dyes, viz. Rhodamine B and Methylene blue, under natural sunlight. Nanoparticles were synthesized using zinc acetate and starch extracted from potato at pH 7–8. Potato starch acts as both a capping agent and a reducing agent. They were characterized spectroscopically via XRD, SEM, HR-TEM, EDAX and FT-IR techniques. Bean/spherical shaped ZnO NPs were obtained in the size range of 29–49 nm whereas calcium coating on ZnO decreased the particle size, i.e., 25–35 nm. Their photocatalytic ability to degrade Rhodamine B and Methylene blue was studied under natural sunlight and monitored using UV-Vis spectrophotometer. Synthesized ZnO nanoparticles and its calcium coated ZnO nanocomposites showed promising results in degradation of these dyes. Methylene blue was completely degraded in an hour at 8 mg of the sample. Although degradation of Rhodamine dye was slow, synthesized samples were effective catalysts as compared to the ones reported in the literature.

Keywords: ZnO NPs; Ca-ZnO Nanocomposites; Potato Starch; Methylene Blue; Rhodamine B

ARTICLE INFO

Received: 25 March 2023
Accepted: 17 May 2023
Available online: 6 July 2023

1. Introduction

World appears as an aesthetic place due to the colours in the surrounding. These are either natural or man-made. The key component that renders colours around us is dyes. Dyes are primarily responsible for the colour of fabrics and drugs. Dyeing process requires a massive amount of water for processing and activation of colour. There are several industries like tanneries, food processing, cosmetics, textile, and pharmaceuticals that discharge toxic contaminants[1,2]. Textile industries are mainly responsible for water pollution as they discharge unwanted effluents and release that in nearby water bodies. Moreover, in some cases, wastewater is directly used for irrigation purposes that is dangerous to edible crops as well as to soil. Rapid industrialization has led to the tremendous production of dye loaded wastewater in the past few

years. The major problems associated with the dye pollution are high demand for fashion, complex nature of dyes, poorly managed industries and moreover their non-biodegradable nature make them to last long in the environment producing several hazards[3]. Rhodamine B and Methylene blue dyes are frequently used in textile, paint & pigment industries and medical area[4]. If we look around, we see that water bodies have turned blue, green, red and even black when dye concentration is many more times. Due to which these water bodies have been declared dead. Their presence in water has severely affected aquatic life and causes several health issues such as eye and skin problems, palpitation of heart and even has been identified as cancer-causing agents[5,6]. Hence, dye removal from wastewater is needed before discharging into the environment. Several approaches have been reported for the treatment of dye loaded water such as adsorption, coagulation, filtration, and AOPs. Nanomaterials have been widely used as filters, adsorbents, membranes etc. in the wastewater treatment[7,8]. Their response towards environment depends upon various parameters like temperature, range of sunlight, pH[9,10]. Photocatalysis is a viable and sustainable process to remove dyes from waste water[11–13]. Photocatalysis is the reaction induced by the UV-Visible light when falls over the surface of semiconducting materials. Heterogeneous photocatalysts based on semiconductors, such as TiO_2, ZnO and ZnS, have received much attention for the use of solar energy in solving environmental problems[14]. Morphology of the photocatalyst has a remarkable role in such reactions. Among all, zinc oxide is very common semiconductor with a wide band gap (3.27 eV) at room temperature and high exciton binding energy. Owing to exceptional properties such as environment safe, economical, non-toxic, and stability, zinc oxide nanoparticles have been used in several fields especially cosmetics and catalysis[15,16]. The photocatalytic efficiency is also improved by coating the ZnO catalyst surface with Au, Ag, Cu, etc.[17–19]. Zinc oxide nanoparticles have been synthesized by various top down and bottom-up approaches[20–23]. Biological approaches using plants sources for nanoparticle synthesis seem to be the valuable alternatives to chemical methods[24]. Potato is a tuberous crop and rich in starch content. Starch is a natural polymer, abundant in nature, economical, renewable and moreover easily available. Starch, on hydrolysis produces amylose (linear polymer) and amylopectin (cross-linked polymer), these two polymers due to their interaction form a molecular capsule which can act as a template for the growth of NPs[25,26]. Calcium oxide is considered to be sustainable photocatalyst so combination of two might result in an effective photocatalyst[27]. CaO NPs have higher surface area that led to higher adsorption of dyes on their surface. In the present article, we present a simple and one-pot green method for the synthesis of ZnO nanoparticles (NPs) and Ca-ZnO nanocomposites using potato starch. Photocatalytic activity of the samples was studied by degradation of two organic dyes, Methylene blue and Rhodamine B[28–30].

2. Materials and methodology

2.1 Chemicals

Zinc acetate dihydrate ($Zn(CH_3COO)_2{\cdot}2H_2O$), Calcium chloride ($CaCl_2$) and sodium hydroxide (NaOH) were of analytical grade (99% purity) and purchased from Merck, India. Methylene blue and Rhodamine B were purchased from Sigma-Aldrich. Deionized (DI) water was used to prepare solution and extract.

2.2 Preparation of potato starch

Potatoes were bought from the local market. They were washed several times with DI water to remove dirt. About 10 g was cut into small pieces and then boiled in 100 mL of DI water for 15 min. After cooling, the solution was centrifuged to remove the insoluble fraction. The cloudy solution was then stored in glass bottles and refrigerated for later use.

2.3 Preparation of zinc oxide nanoparticles (POP)

40 mL of potato starch extract was taken in a 100 C.C beaker containing a magnetic bead. The solution was heated to a temperature of 60–70 °C, followed by addition of zinc salt. The pH of the solution was maintained in the range of 7.5–8.0 (with NaOH)[31,32]. It was stirred at this temperature for 30–40 min until a pale-yellow precipitate was formed. The resulting solution was centrifuged and then washed with DI water, followed by drying

in an oven at 80 °C. The dried powder was then cal-cined at 500 °C in a muffle furnace for 15 min. The synthesized sample was named as POP and stored for further analysis.

2.4 Preparation of Ca-ZnO nanocomposites (POP11 and POP21)

Ca-ZnO nanocomposites were prepared by coprecipitation method. To synthesize Ca-ZnO nanocomposites, desired amount of Zn salt was dissolved in potato starch (extract) taken in a beaker at temperature 60 °C. The pH of the solution was maintained in the range of 7–8 by adding sodium hydroxide solution. Solution was stirred for half an hour to reduce the zinc salt to the metallic Zn at the maintained temperature. Calcium salt in two different weight ratios (Zn:Ca = 1:1 and 2:1) was then added in small lots with continuous stirring. Resulting solution was stirred for nearly an hour and NPs were collected by centrifugation. They were washed with DI water to do away with the impurities and dried in oven. It was calcinated at 500 °C in a muffle furnace for 15 min (**Figure 1**). The Ca-ZnO nanocomposites prepared in 1:1 and 2:1 ratio was named as POP11 and POP21, respectively.

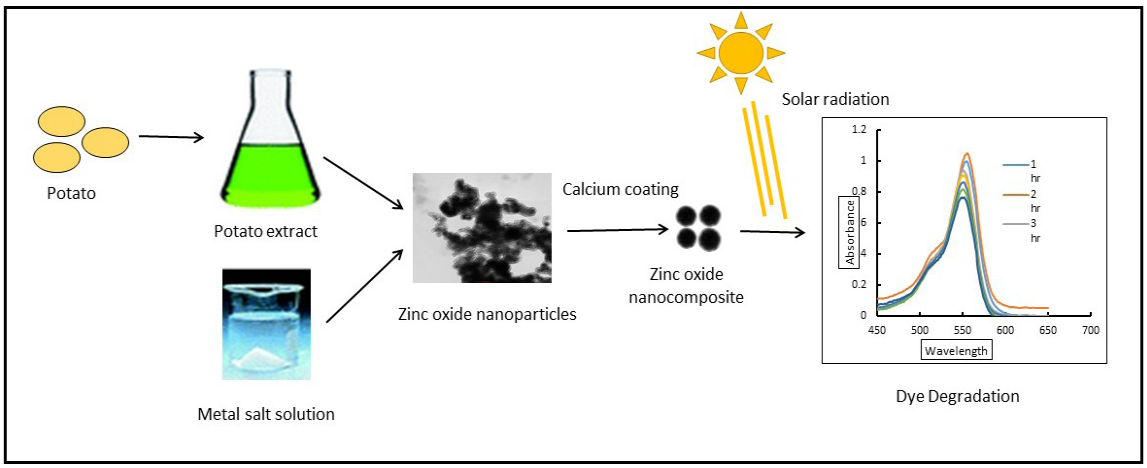

Figure1. Graphical representation of starch mediated coated and uncoated ZnO NPs and their photocatalytic activity towards dye degradation.

A hypothetical mechanism for the formation of Ca-ZnO nanocomposites is given in. Equation (1). The samples were stored for further analysis.

$$Zn(OCOCH_3)_2 + NaOH + CaCl_2\ Potato\ Starch \rightarrow Zn(OH)_2 + NaOAc + Ca^{2+} + 2Cl^- \rightarrow Ca - ZnO\ nanocomposites \quad (1)$$

2.5 Characterization of ZnO NPs and Ca-ZnO nanocomposites

The samples were obtained as white/off white solids. They were characterized by SEM coupled with EDAX, HR-TEM, FT-IR and XRD. Absorbance was determined with a UV-Vis spectrophotometer (Motras) in the range of 200–800 nm. Crystalline phases of the synthesized ZnO NPs and its calcium nanocomposites were characterized by an X-ray diffractometer recorded with a Bruker, D8 Discover X-ray source supplied with Cu 2-theta in the range of 10°–90°. The morphology and size of the synthesized ZnO NPs and their nanocomposites were investigated by scanning electron microscopy (SEM), energy dispersive X-ray analysis (EDAX) (JEOL JSM-6610LV) and high-resolution electron microscopy (HR-TEM) (Thermo Fischer Scientific Talos L120C). FT-IR was recorded on a Nicolet iS50 FT-IR between 4,000 and 400 cm^{-1} to determine the nature of the functional groups of the nanoparticles and their nanocomposites.

2.6 Photocatalytic activity

The photocatalytic properties of the synthesized samples were determined by the degradation of Rhodamine B (RB) and Methylene blue (MB) dyes. First, a dye solution was prepared by dissolving 10 mg of the respective dye in 1 L of deionized (DI) water. Weighed amount (2/4/8 mg) of the synthesized ZnO NP/Ca-ZnO nanocomposites was added to 100 mL of the corresponding dye solution taken in 250 C.C. Erlenmeyer flask. Controls for both dyes were also prepared without samples. The solution was stirred with a magnetic stirrer for

15 min to reach equilibrium. It was then exposed to sunlight and observed until sunlight reached its maximum (usually 6–7 h). The solution was shaken occasionally. Aliquots of 2–3 mL were taken at certain time intervals and the photocatalytic degradation activity was determined. The absorption spectrum of the supernatant was measured with a UV-visible spectrophotometer at different wavelengths. The concentration of the dye at different time intervals was calculated by measuring the absorbance value of Methylene blue at 627 nm and the absorbance value of Rhodamine B at approx. 554 nm.

The percentage of dye degradation was determined by the following formula:

$$\%\ of\ Dye\ Degradation = \frac{(C_0 - C)}{C_0} \times 100 \quad (2)$$

C_0 = initial concentration of dye, C = concentration of dye at a particular time interval.

3. Results and discussion

3.1 XRD

Potato starch mediated ZnO nanoparticles (**Figure 1(a)**) have characteristics peaks at 32.08° (100), 36.28° (002), 36.57° (101), 47.89° (102), 56.77° (110), 63.04° (103), 68.19° (201) that represents hexagonal wurtzite structure of ZnO. Intensity of the ZnO peak at 36.57° (101) was higher than the intensities of the other peaks, indicating a considerable growth of NPs. The XRD pattern shows that prepared calcium nanocomposites of ZnO also have hexagonal wurtzite structure. In calcium coated ZnO nanoparticles, growth mainly took place in the (101) plane, although intensities of peaks at (002) and (100) have somewhat become more intense as compared to ZnO NPs (**Figure 2(a)**). Also, there is an additional diffraction peak appeared at 29.46° characteristics of Ca. This confirms the incorporation of calcium ion into ZnO lattice. It is noteworthy that calcium coating did not affect the crystallinity of ZnO with a wurtzite structure[33].

3.2 FT-IR

The FT-IR spectra of ZnO nanoparticles and its calcium nanocomposites (**Figure 2(b)**) reveals the capping/stabilizing agents found in potato starch. Spectra shows a broad band at 3,437 cm^{-1} associated with O-H stretching of starch present in potato. This band diminished in case of POP11 and POP21 indicating their involvement in the nanocomposite synthesis. The characteristics peak due to C=O group appeared at 1,614 cm^{-1}. The spectrum represents a weak peak near to 459 cm^{-1} corresponds to ZnO[34–36].

3.3 SEM (scanning electron microscopy) and HR-TEM (high-resolution transmission electron microscope)

Validation of the XRD result was verified by the SEM (scanning electron microscope) and HR-TEM (high-resolution transmission electron microscope). Shape and surface morphology of the zinc oxide nanoparticles and their calcium nanocomposites, POP11 and POP21 are displayed in **Figure 3(a–c)** and **Figure 4(a–f)**. ZnO nanoparticles (POP) showed aggregated morphology made up of many more likely to be beans shaped uniform particles. The coating of calcium ions into the crystalline structure could change the morphology which is clear in the SEM and TEM images. Incorporation of calcium into ZnO did not change the

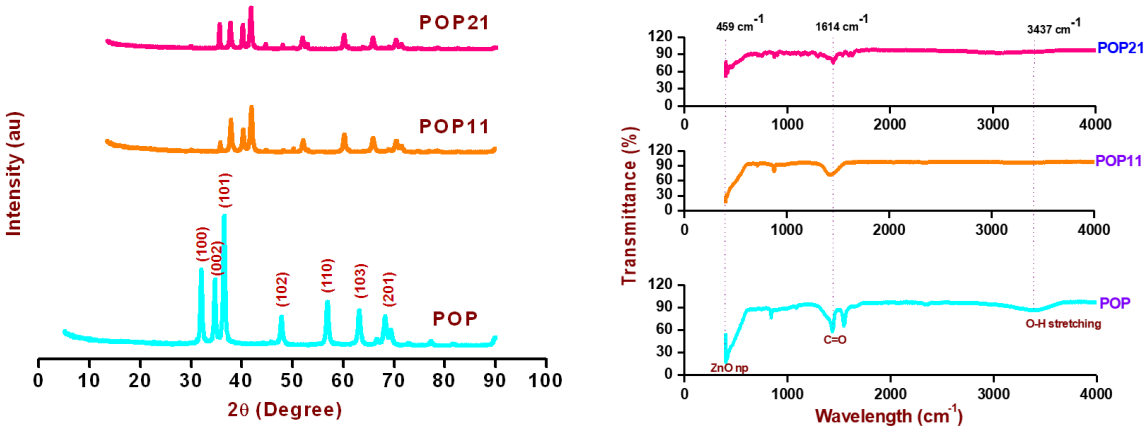

(a) (b)

Figure 2. (a) XRD pattern of ZnO NPs (POP) and Ca- ZnO (POP11 & POP21) and (b) FT-IR spectrum of POP, POP11 and POP21.

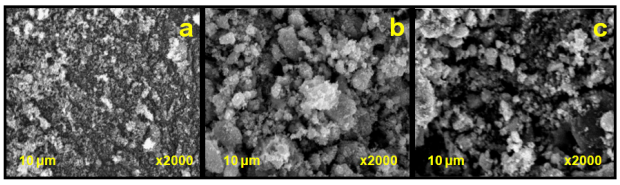

Figure 3. SEM images of (a) POP (b) POP11 and (c) POP21.

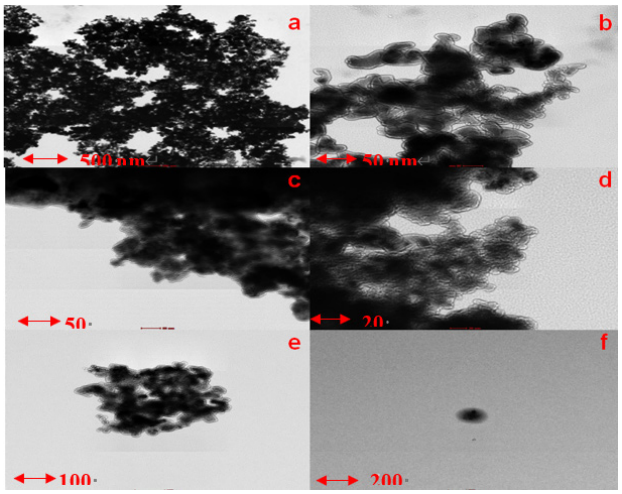

Figure 4. HR-TEM images of (a & b) potato starch mediated ZnO NPs (POP) (c & d) POP11 and (e & f) POP21.

morphology of the Ca-ZnO nanocomposites at low magnification. But at a higher magnification, there was more aggregation observed than uncoated ZnO NPs consistent with the results reported in the literature and they were likely spherical in shape[37]. It is significant to note that the lack of uniformity can be further explained by the accumulation of ZnO nanoparticles and the formation of irregular crystals during the synthesis process. The particle size in ZnO nanoparticles ranges from 29–49 nm whereas in case of Ca-ZnO nanocomposites, the particle size ranges between 72–89 nm for POP11 and 25–35 nm for POP21.

3.4 EDS and element mapping

Elemental analysis and elemental mapping of the samples were performed by EDAX/EDS. EDAX images confirms the presence of Zn, O and Ca elements as elemental constituents of the synthesized nanoparticles/nanocomposites. EDAX images of ZnO nanoparticles indicates the presence of Zn and O atoms in a stoichiometric ratio (**Figure 5(a)**). EDS images of Ca-ZnO nanocomposites shows that Ca is present in the nanostructure in addition to Zn and O (**Figure 5(b)** and **(c)**). Moreover, no impurity peaks were found in POP (according to the results), indicating the high purity of the synthesized sample. Although traces of chlorine can be seen in POP11 and POP21 which might not be removed during washing (due to the use of calcium chloride salt in nanocomposites preparation). Furthermore, weight percentages of Zn and O were 60.11 and 39.89 in POP. Weight percentages of Zn, O and Ca elements in POP11 were found to be 58.04, 32.29 and 9.67 and in POP21, they were 71.45, 24.56 and 3.27 along with trace of chlorine[38].

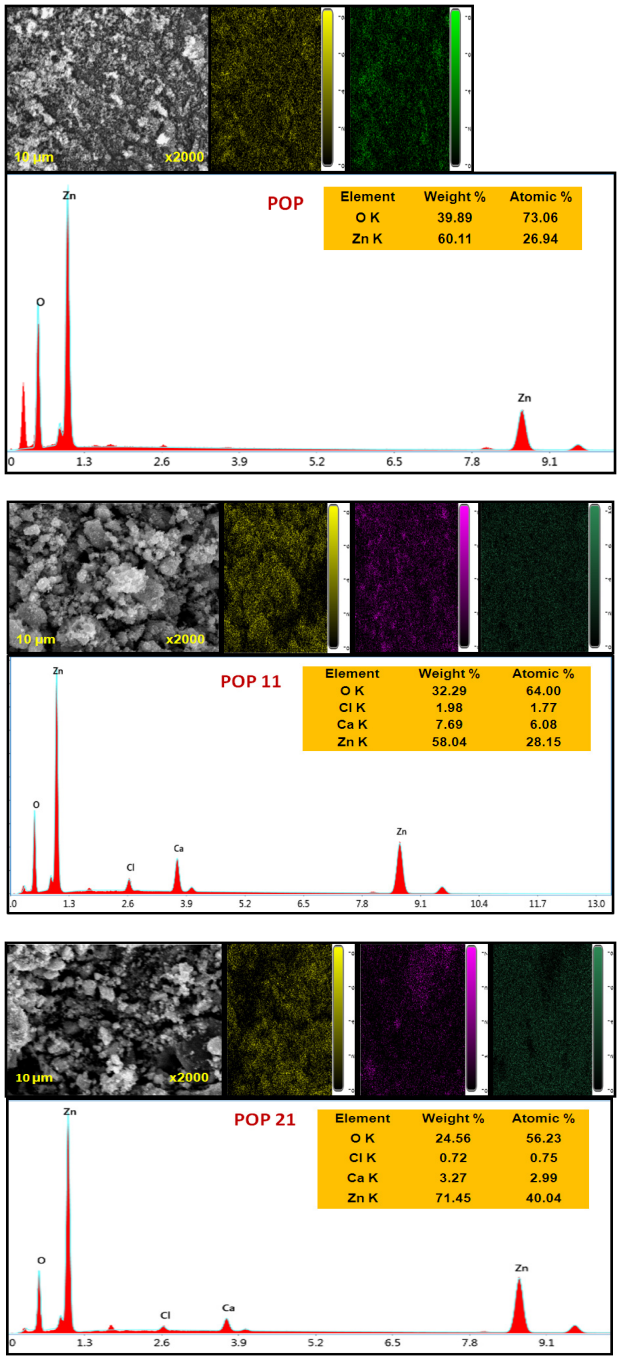

Figure 5. EDS image and element mapping of (a) POP (b) POP11 and (c) POP21.

3.5 Photocatalytic activity of Methylene blue and Rhodamine B

Photocatalytic reactions involve electron-hole pair formation by semiconductor NPs. When irradiated with sunlight, the absorbed photons can cause electrons to be excited from the valence band (VB) to the conduction band (CB) to produce an electron and a hole. These species then generate oxidizing agents such as H_2O_2, O_2^- , OH^- after interaction with oxygen and water on the surface of the ZnO. These are strong oxidizing agents and can decompose organic dyes into carbon dioxide and water (Equations (3–8))[39,40].

$$ZnO + Sunlight \rightarrow ZnO\left(e^- + h^+\right) \quad (3)$$

$$H_2O + h^+ \rightarrow OH + H^+ \quad (4)$$

$$O_2 + e^- \rightarrow O_2^- \quad (5)$$

$$2H^+ + 2O_2 \rightarrow H_2O_2 + O_2 \quad (6)$$

$$H_2O_2 + light \rightarrow 2OH^- \quad (7)$$

$$OH^- + dye \rightarrow CO_2 + H_2O \quad (8)$$

Figure 6 shows the effect of ZnO NPs and its calcium nanocomposites (1:1 and 2:1) on photodegradation of MB (Methylene blue) and Rh B (Rhodamine B) dyes under natural sunlight. According to Lambert Beer's law, the concentration of dye is directly proportional to its absorbance. Degradation of Methylene blue dye by potato-mediated ZnO NPs and its calcium composites was investigated, and the results are shown in **Figure 6(a–c)**. Degradation of Methylene blue was studied as the disappearance of the peak nearly at 627 nm. In all the cases, blue colour of the Methylene blue was faded by 17%–20% in just 1 h[41]. It almost became colourless after 5 h which is clear from **Figure 6(a–c)**. Similar trend was observed in the case of Rhodamine B. Coating of calcium on the surface of ZnO nanoparticles increased the degradation of Methylene blue and Rhodamine B as evident in POP21. Higher concentration of calcium (in case of POP11) did not have much impact on degradation of Methylene blue. The degradability of a Rhodamine B dye was monitored by change in its absorption peak at 554 nm. As evident from the figure, the degradation efficiency of the Rhodamine B dye by synthesized ZnO NPs and its calcium composite increased with time[42–44]. Although, it has been reported that Rhodamine B dye degrades very slowly, our synthesized samples could effectively degrade it (**Figure 6(d–f)**). Degradation efficiency of Rhodamine B was nearly in the range of 29%–31% for POP and POP11 nanocomposite but higher in case of POP(21), i.e., 36% after 7 h[45]. MB and Rh B are cationic dyes and their adsorption by the synthesized sample is indicating negatively charged

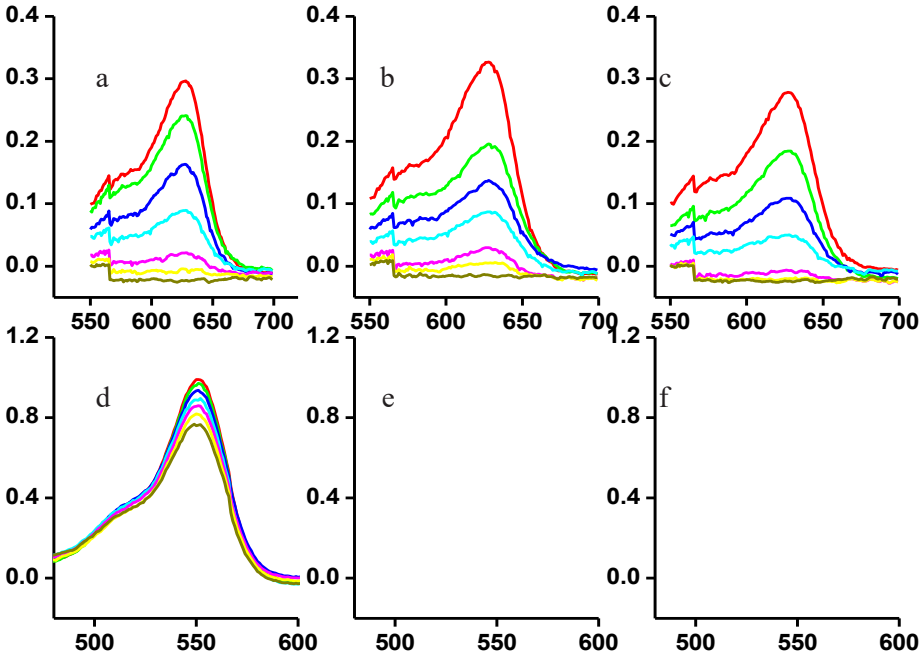

Figure 6. UV-Vis spectra of degradation of Methylene blue by (a) POP (b) POP11 (c) POP21 and UV-Vis spectra of degradation of Rhodamine B by (d) POP (e) POP11 (f) POP21 at different time intervals in presence of solar light.

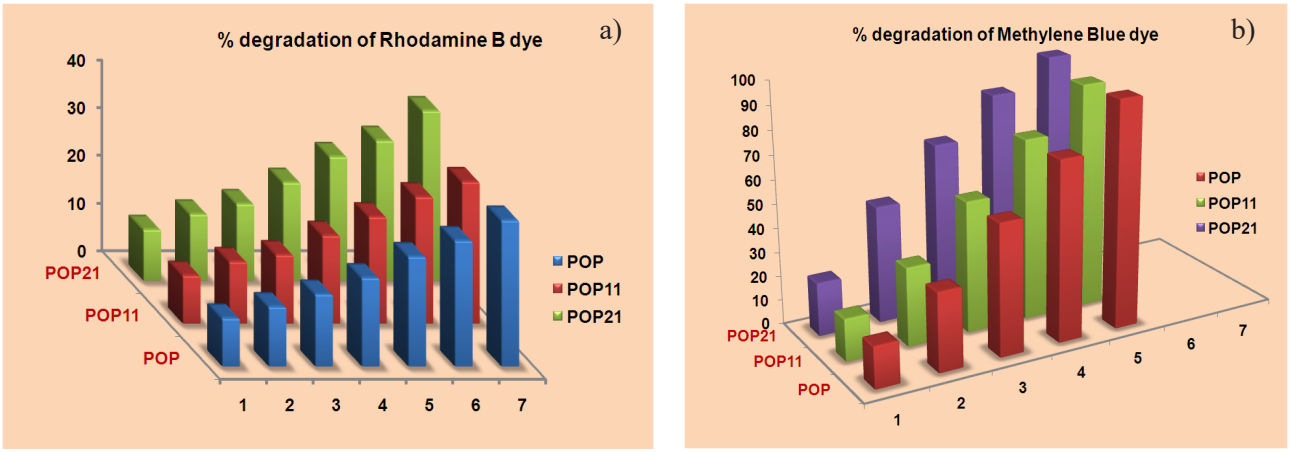

Figure 7. a) % Degradation of Rhodamine B; b) % Degradation of Methylene blue by ZnO nanoparticles (POP) and its nanocomposites (POP11 and POP21).

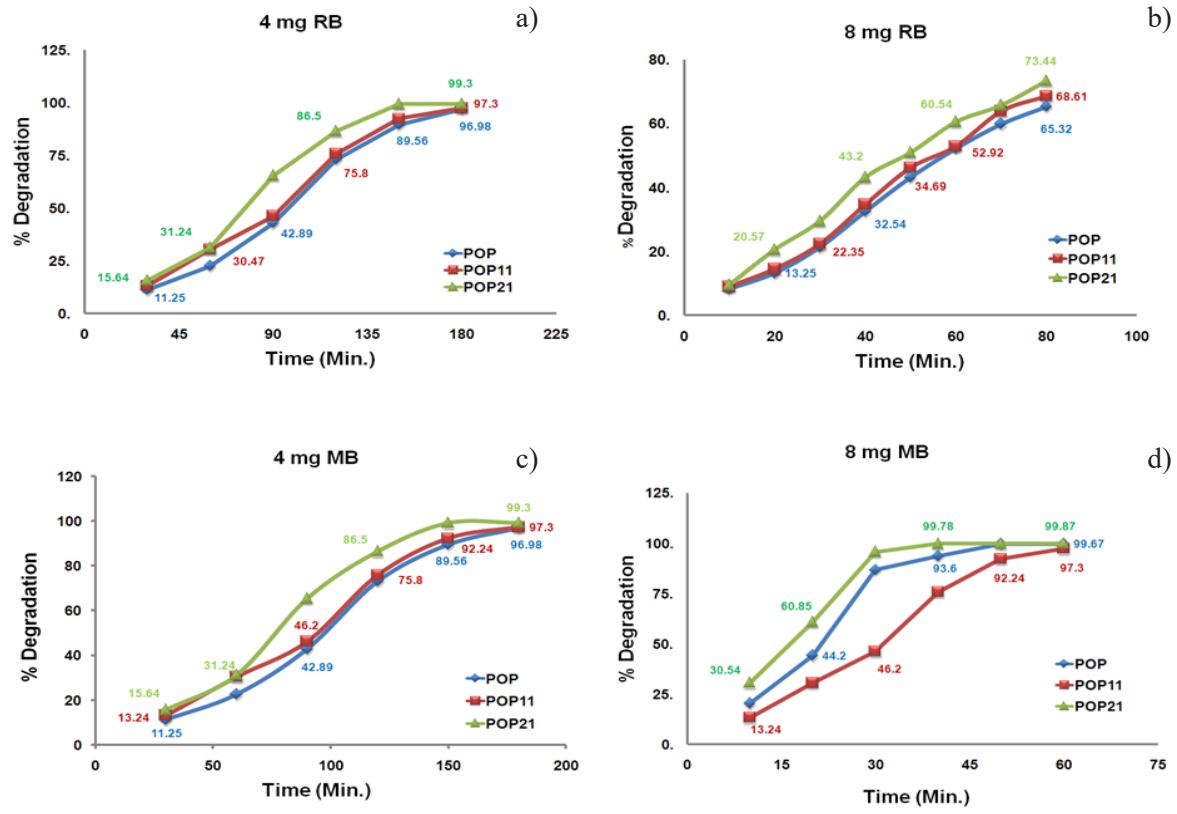

Figure 8. % degradation of RB at a) 4 mg concentration; b) 8 mg concentration of POP/POP11/POP21 and % degradation of MB at c) 4 mg concentration; d) 8 mg concentration of POP/POP11/POP21.

surface of the synthesized samples[46]. Comparison between degradation efficiency of two dyes has been shown in **Figure 7**.

3.6 Effect of concentration of POP/ POP11/POP21

The impact of concentration of POP/POP11/ POP21 on dye degradation was also studied by UV-Vis spectrophotometer. The degradation of dyes became faster on increasing the concentration of the POP/POP21/POP11 **(Figure 8)**. When 4 mg of synthesized samples was added in 100 mL of Rhodamine B dye solution (constant volume) under natural sunlight, the dye degradation was enhanced to nearly 90% in 180 min whereas it was approximately 70% in case of 8 mg sample suspended in the same volume of dye solution in 80 min. Similarly, blue color of the Methylene blue dye was completely vanished in just 30 min when 8 mg of sample was suspended in the dye solution. Observed results confirmed that synthesized ZnO nanoparticles and its calcium composites are very

effective photodegradation of Methylene blue and Rhodamine B[47,48].

4. Conclusion

Potato starch mediated ZnO nanoparticles and its calcium composites (POP11 and POP21) were successfully synthesized by simple and one pot method. They were investigated by FT-IR, HRTEM, XRD, SEM-coupled EDAX, etc. HR-TEM images revealed that bean as well as spherical shaped nanoparticles in the size range of 29–49 nm were obtained in the present method. However, coating of calcium (2:1) had decreased the particle size but further rise in calcium amount (1:1 ratio) had led to increase in the size of the nanoparticles. The XRD pattern showed that coated and uncoated ZnO NPs have stable hexagonal wurtzite structure. EDS images showed the presence of Zn, O and Ca elements in the synthesized samples. They could degrade the Methylene blue completely and Rhodamine B up to 38% under natural sunlight when just 2 mg was suspended in 100 mL dye solution in 6–7 h. At 8 mg of the samples, dye solutions were completely decolorized. These results indicate their potential in the deterioration of toxic organic compounds in wastewater.

Acknowledgements

The authors are grateful to Daulat Ram College, University of Delhi for providing the necessary laboratory infrastructure to carry out the experimental work. We sincerely thank USIC Department of Chemistry, DU Universities and Jamia Hamdard for sample characterization.

Authors contribution

Analysis proposal, design and synthesis: DS; data collection: A and AK; data analysis: SK; writing: RK; data writing and analysis: ND and SK; investigation and revision: MRS and IPS.

Conflict of interest

The authors declare that there is no conflict of interest.

References

1. Samuchiwal S, Gola D, Malik A. Decolourization of textile effluent using native microbial consortium enriched from textile industry effluent. Journal of Hazardous Materials 2021; 402: 123835. doi: 10.1016/j.jhazmat.2020.123835.
2. Bansal M, Patnala PK, Dugmore T. Adsorption of Eriochrome Black-T(EBT) using tea waste as a low cost adsorbent by batch studies: A green approach for dye effluent treatments. Current Research in Green and Sustainable Chemistry 2020; 3: 100036. doi: 10.1016/j.crgsc.2020.100036.
3. Nazir MA, Bashir MS, Jamshaid M, *et al*. Synthesis of porous secondary metal-doped MOFs for removal of Rhodamine B from water: Role of secondary metal on efficiency and kinetics. Surfaces and Interfaces 2021; 25: 101261. doi: 10.1016/j.surfin.2021.101261.
4. Wang S, Zhu ZH. Characterisation and environmental application of an Australian natural zeolite for basic dye removal from aqueous solution. Journal of Hazardous Materials 2006; 136(3): 946–952. doi: 10.1016/j.jhazmat.2006.01.038.
5. Wan D, Li W, Wang G, *et al*. Adsorption and heterogeneous degradation of Rhodamine B on the surface of magnetic bentonite material. Applied Surface Science 2015; 349: 988–996. doi: 10.1016/j.apsusc.2015.05.004.
6. Sinha T, Ahmaruzzaman M, Bhattacharjee A. A simple approach for the synthesis of silver nanoparticles and their application as a catalyst for the photodegradation of methyl violet 6B dye under solar irradiation. Journal of Environmental Chemical Engineering 2014; 2(4): 2269–2279. doi: 10.1016/j.jece.2014.10.001.
7. Sinha T, Ahmaruzzaman M. High-value utilization of egg shell to synthesize Silver and Gold−Silver core shell nanoparticles and their application for the degradation of hazardous dyes from aqueous phase—A green approach. Journal of Colloid and Interface Science 2015; 453: 115–131. doi: 10.1016/j.jcis.2015.04.053.
8. Ahmad A, Mohd-Setapar SH, Chuong CS, *et al*. Recent advances in new generation dye removal technologies: Novel search for approaches to reprocess wastewater. RSC Advances 2015; 5: 30801–30818. doi: 10.1039/c4ra16959j.
9. Dong S, Feng J, Fan M, *et al*. Recent developments in heterogeneous photocatalytic water treatment using visible light-responsive photocatalysts: A review. RSC Advances 2015; 5: 14610–14630. doi: 10.1039/C4RA13734E.
10. Nazir MA, Khan NA, Cheng C, *et al*. Surface induced growth of ZIF-67 at Co-layered double hydroxide: Removal of Methylene blue and methyl orange from water. Applied Clay Science 2020; 190: 105564. doi: 10.1016/j.clay.2020.105564.
11. Nazir MA, Najam T, Shahzad K, *et al*. Heteroint-

erface engineering of water stable ZIF-8@ZIF-67: Adsorption of Rhodamine B from water. Surfaces and Interfaces 2022; 34: 102324. doi: 10.1016/j.surfin.2022.102324.
12. Nazir MA, Nazam T, Jabeen S, *et al*. Facile synthesis of tri-metallic layered double hydroxides (NiZnAl-LDHs): Adsorption of Rhodamine-B and methyl orange from water. Inorganic Chemistry Communications 2022; 145: 110008. doi: 10.1016/j.inoche.2022.110008.
13. Momeni MM. Study of synergistic effect among photo-, electro-, and sonoprocesses in photocatalyst degradation of phenol on tungsten-loaded titania nanotubes composite electrode. Applied Physics A: Materials Science and Processing 2015; 119: 1413–1422. doi: 10.1007/s00339-015-9114-3.
14. Liqiang J, Yichun Q, Baiqi W, *et al*. Review of photoluminescence performance of nano-sized semiconductor materials and its relationships with photocatalytic activity. Solar Energy Materials and Solar Cells 2006; 90(12): 1773–1787. doi: 10.1016/j.solmat.2005.11.007.
15. Mahlambi MM, Ngila CJ, Mamba BB. Recent developments in environmental photocatalytic degradation of organic pollutants: The case of titanium dioxide nanoparticles—A review. Journal of Nanomaterials 2015; 2015: 790173. doi: 10.1155/2015/790173.
16. Ruszkiewicz JA, Pinkas A, Ferrer B, *et al*. Neurotoxic effect of active ingredients in sunscreen products, a contemporary review. Toxicology Reports 2017; 4: 245–259. doi: 10.1016/j.toxrep.2017.05.006.
17. Guy N, Çakar S, Ozacar M. Comparison of palladium/zinc oxide photocatalysts prepared by different palladium doping methods for congo red degradation. Journal of Colloid and Interface Science 2016; 466: 128–137. doi: 10.1016/j.jcis.2015.12.009.
18. Rodrigues J, Hatami T, Rosa JM, *et al*. Photocatalytic degradation using ZnO for the treatment of RB 19 and RB 21 dyes in industrial effluents and mathematical modeling of the process. Chemical Engineering Research and Design 2020; 153: 294–305. doi: 10.1016/j.cherd.2019.10.021.
19. Liu H, Hu Y, Zhang Z, *et al*. Synthesis of spherical Ag/ZnO heterostructural composites with excellent photocatalytic activity under visible light and UV irradiation. Applied Surface Science 2015; 355: 644–652. doi: 10.1016/j.apsusc.2015.07.012.
20. Ul-Haq AN, Nadhman A, Ullah I, *et al*. Synthesis approaches of zinc oxide nanoparticles: The dilemma of ecotoxicity. Journal of Nanomaterials 2017; 2017: 8510342. doi: 10.1155/2017/8510342.
21. Bandeira M, Giovanela M, Roesch-Ely M, *et al*. Green synthesis of zinc oxide nanoparticles: A review of the synthesis methodology and mechanism of formation. Sustainable Chemistry and Pharmacy 2020; 15: 100223. doi: 10.1016/j.scp.2020.100223.
22. Mallakpour S, Madani M. Use of silane coupling agent for surface modification of zinc oxide as inorganic filler and preparation of poly(amide–imide)/zinc oxide nanocomposite containing phenylalanine moieties. Bulletin of Materials Science 2012; 35(3): 333–339. doi: 10.1007/s12034-012-0304-8.
23. Ma J, Zhu W, Tian Y, *et al*. Preparation of zinc oxide-starch nanocomposite and its application on coating. Nanoscale Research Letters 2016; 11: 200. doi: 10.1186/s11671-016-1404-y.
24. Mehmood A, Murtaza G, Bhatti TM, *et al*. Phyto-mediated synthesis of silver nanoparticles from *Melia azedarach* L. leaf extract: Characterization and antibacterial activity. Arabian Journal of Chemistry 2017; 10(2): S3048–S3053. doi: 10.1016/j.arabjc.2013.11.046.
25. Renault F, Morin-Crini N, Gimbert F, *et al*. Cationized starch-based materials a new ion-exchanger adsorbent for the removal of C.I. Acid Blue 25 from aqueous solutions. Bioresource Technology 2008; 99(16): 7573–7586. doi: 10.1016/j.biortech.2008.02.011.
26. Chen Q, Yu H, Wang L, *et al*. Recent progress in chemical modification of starch and its applications. RSC Advances 2015; 5: 67459–67474. doi: 10.1039/c5ra10849g.
27. Sree GV, Nagaraaj P, Kalanidhi K, *et al*. Calcium oxide a sustainable photocatalyst derived from eggshell for efficient photo-degradation of organic pollutants. Journal of Cleaner Production 2020; 270: 122294. doi: 10.1016/j.clepro.2020.122294.
28. Osuntokun J, Onwudiwe DC, Ebenso EE. Aqueous extract of broccoli mediated synthesis of CaO nanoparticles and its application in the photocatalytic degradation of bromocresol green. IET Nanobiotechnology 2018; 12(7): 888–894. doi: 10.1049/iet-nbt.2017.0277.
29. Gopalappa H, Yogendra K, Mahadevan KM, *et al*. A comparative study on the solar photocatalytic degradation of brilliant red azo dye by CaO and $CaMgO_2$ nanoparticles. International Journal of Science and Research 2012; 1: 91–95. doi: 10.13140/RG.2.2.24749.95204.
30. Thakur S, Singh S, Pal B. Time-dependent growth of CaO nano flowers from egg shells exhibit improved adsorption and catalytic activity. Advanced Powder Technology 2021; 32: 3288–3296. doi: 10.1016/j.apt.2021.07.015.

31. Buazara F, Bavi M, Kroushawi F, *et al*. Potato extract as reducing agent and stabiliser in a facile green one-stepsynthesis of ZnO nanoparticles. Journal of Experimental Nanoscience 2016; 11(3): 175–184. doi: 10.1080/17458080.2015.1039610.
32. Singh D, Anuradha, Mathur D, *et al*. Photocatalytic properties of biologically synthesized uncoated and calcium coated ZnO nanoparticles using cucumber juice. Rasayan Journal of Chemistry 2022; Special Issue: 95–102. doi: 10.31788/RJC.2022.1558177.
33. Huang Y, Lyu LM, Lin CY, *et al*. Improved mass-transfer enhances photo-driven dye degradation and H_2 evolution over a few-layer WS_2/ZnO heterostructure. ACS Omega 2022; 7(2): 2217–2223. doi: 10.1021/acsomega.1c05756.
34. Daman TC, Porto SPS, Tell B. Raman effect in zinc oxide. Physical Review 1981; 142: 570. doi: 10.1103/PhysRev.142.570.
35. Richter H, Wang ZP, Ley L. The one phonon Raman spectrum in microcrystalline silicon. Solid State Communications 1981; 39(5): 625–629. doi: 10.1016/0038-1098(81)90337-9.
36. Abebe B, Zereffa EA, Murthy HCA. Synthesis of poly(vinyl alcohol)-aided ZnO/Mn_2O_3 nanocomposites for acid orange-8 dye degradation: Mechanism and antibacterial activity. ACS Omega 2021; 6(1): 954–964. doi: 10.1021/acsomega.0c05597.
37. Pham TAT, Tran VA, Le VD, *et al*. Facile preparation of ZnO nanoparticles and Ag/ZnO nanocomposite and their photocatalytic activities under visible light. International Journal of Photoenergy 2020; 2020: 8897667. doi: 10.1155/2020/8897667.
38. Yontar AK, Avcioglu S, Cevik S. Nature-based nanocomposites for adsorption and visible light photocatalytic degradation of Methylene blue dye. Journal of Cleaner Production 2022; 380: 135070. doi: 10.1016/j.jclepro.2022.135070.
39. Muruganandham M, Swaminathan M. Photocatalytic decolorization and degradation of reactive orange 4 by TiO_2-UV process. Dyes and Pigments 2006; 68(2–3): 133–142. doi: 10.1016/j.dyepig.2005.01.004.
40. Al Hamedi FH, Rauf MA, Ashraf SS. Degradation studies of Rhodamine B in the presence of UV/H_2O_2. Desalination 2009; 239(1–3): 159–166. doi: 10.1016/j.desal.2008.03.016.
41. Batra V, Kaur I, Pathania D, *et al*. Efficient dye degradation strategies using green synthesized ZnO-based nanoplatforms: A review. Applied Surface Science Advances 2022; 11: 100314. doi: 10.1016/j.apsadv.2022.100314.
42. Jeffrey A, Nethravathi C, Rajamathi M. Nitrogen-doped alkylamine-intercalated layered titanates for photocatalytic dye degradation. ACS Omega 2019; 4(1): 1575–1580. doi: 10.1021/acsomega.8b03207.
43. Vijayan K, Vijayachamundeeswari SP. Improving the multifunctional attributes and photocatalytic dye degradation of MB and RhB dye—A comparative scrutiny. Inorganic Chemistry Communications 2022; 144: 109940. doi: 10.1016/j.inoche.2022.109940.
44. Gul R, Sharma P, Kumar R, *et al*. A sustainable approach to the degradation of dyes by fungal species isolated from industrial wastewaters: Performance, parametric optimization, kinetics and degradation mechanism. Environmental Research 2023; 216: 114407. doi: 10.1016/j.envres.2022.114407.
45. Shaheen I, Ahmed KS, Thomas A, *et al*. Phytogenic synthesis and enhanced photocatalytic properties of $ZnOCo_3O_4$ p-n junction: Biomimetic water remediators. Ionics 2022; 28: 1999–2006. doi: 10.1007/s11581-021-04407-0.
46. Abhilash MR, Akshatha G, Srikantaswamy S. Photocatalytic dye degradation and biological activities of the Fe_2O_3/Cu_2O nanocomposite. RSC Advances 2019; 9: 8557–8568. doi: 10.1039/C8RA09929D.
47. Vo HT, Nguyen AT, Tran CV, *et al*. Self-assembly of porphyrin nanofibers on ZnO nanoparticles for the enhanced photocatalytic performance for organic dye degradation. ACS Omega 2021; 6: 23203–23210. doi: 10.1021/acsomega.1c02808.
48. Reddy NR, Reddy PM, Jung JH, *et al*. Construction of various morphological ZnO-NiO S-scheme nanocomposites for photocatalytic dye degradation. Inorganic Chemistry Communications 2022; 146: 110107. doi: 10.1016/j.inoche.2022.110107.